Nonlinear consolidation in randomly heterogeneous highly compressible aquitards

Berenice Zapata-Norberto, Eric Morales-Casique & Graciela S. Herrera

Hydrogeology Journal
Official Journal of the International Association of Hydrogeologists

ISSN 1431-2174
Volume 26
Number 3

Hydrogeol J (2018) 26:755-769
DOI 10.1007/s10040-017-1698-6

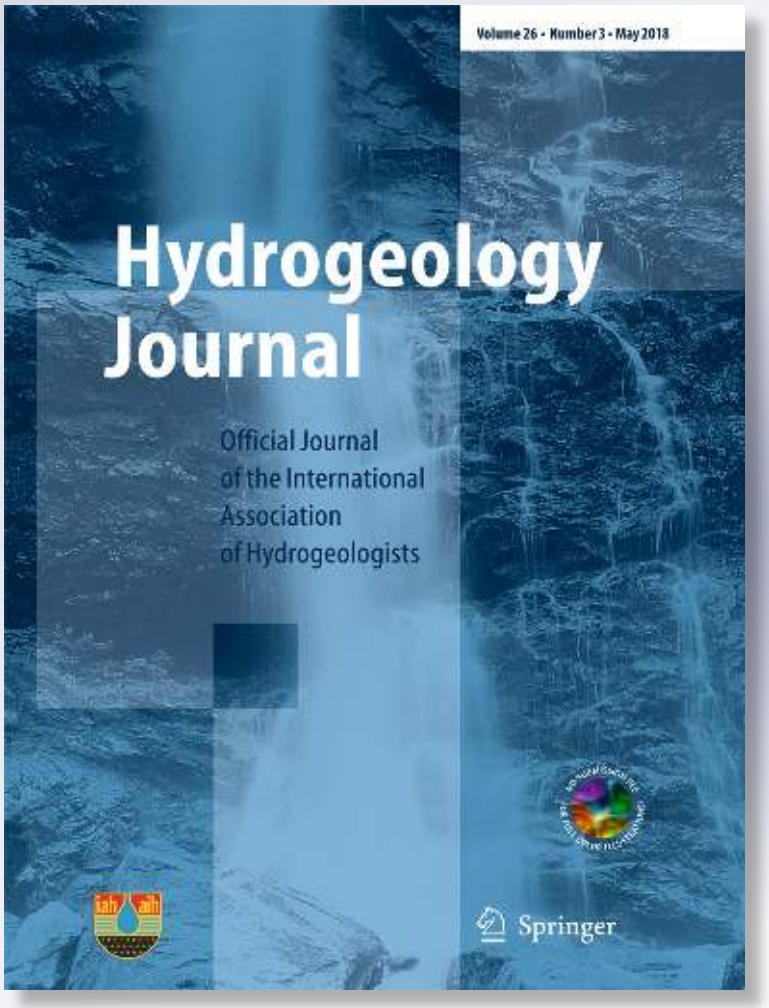

Springer

Your article is protected by copyright and all rights are held exclusively by Springer-Verlag GmbH Germany, part of Springer Nature. This e-offprint is for personal use only and shall not be self-archived in electronic repositories. If you wish to self-archive your article, please use the accepted manuscript version for posting on your own website. You may further deposit the accepted manuscript version in any repository, provided it is only made publicly available 12 months after official publication or later and provided acknowledgement is given to the original source of publication and a link is inserted to the published article on Springer's website. The link must be accompanied by the following text: "The final publication is available at link.springer.com".

Author's personal copy

Hydrogeology Journal (2018) 26:755–769
https://doi.org/10.1007/s10040-017-1698-6

PAPER

Nonlinear consolidation in randomly heterogeneous highly compressible aquitards

Berenice Zapata-Norberto[1] · Eric Morales-Casique[2] · Graciela S. Herrera[3]

Received: 8 May 2017 / Accepted: 19 November 2017 / Published online: 4 December 2017
© Springer-Verlag GmbH Germany, part of Springer Nature 2017

Abstract

Severe land subsidence due to groundwater extraction may occur in multiaquifer systems where highly compressible aquitards are present. The highly compressible nature of the aquitards leads to nonlinear consolidation where the groundwater flow parameters are stress-dependent. The case is further complicated by the heterogeneity of the hydrogeologic and geotechnical properties of the aquitards. The effect of realistic vertical heterogeneity of hydrogeologic and geotechnical parameters on the consolidation of highly compressible aquitards is investigated by means of one-dimensional Monte Carlo numerical simulations where the lower boundary represents the effect of an instant drop in hydraulic head due to groundwater pumping. Two thousand realizations are generated for each of the following parameters: hydraulic conductivity (K), compression index (C_c), void ratio (e) and m (an empirical parameter relating hydraulic conductivity and void ratio). The correlation structure, the mean and the variance for each parameter were obtained from a literature review about field studies in the lacustrine sediments of Mexico City. The results indicate that among the parameters considered, random K has the largest effect on the ensemble average behavior of the system when compared to a nonlinear consolidation model with deterministic initial parameters. The deterministic solution underestimates the ensemble average of total settlement when initial K is random. In addition, random K leads to the largest variance (and therefore largest uncertainty) of total settlement, groundwater flux and time to reach steady-state conditions.

Keywords Nonlinear consolidation · Groundwater flow · Heterogeneity · Monte Carlo · Stochastic modeling

Introduction

Land subsidence refers to both gentle downward displacement and the sudden sinking of parts of the ground surface. It can be due to natural processes (such as mineral dissolution), human activities or a combination of both; however, perhaps the best known cause of subsidence is the extraction of fluids such as water, crude oil and natural gas. The extraction of groundwater can generate land subsidence by causing the compaction of susceptible aquifer systems (Galloway and Burbey 2011). This problem is particularly found in systems with the presence of aquitards (Meade 1967; Poland and Davis 1969; Galloway and Burbey 2011). Theories have been developed to describe and simulate consolidation in multi-layer aquifer systems (Verruijt 1969; Herrera and Figueroa 1969; Herrera 1970; Witherspoon and Freeze 1972; Helm 1972, 1975, 1976; Herrera and Rodarte 1973; Gambolati and Freeze 1973; Herrera and Yates 1977; Narasimhan and Witherspoon 1977; Sandhu 1979; Neuman et al. 1982; Cruickshank-Villanueva 1984; Rivera et al. 1991; Hsieh 1996; Burbey and Helm 1999; Burbey 2005). Several of these theories assume a quasi-three-dimensional (3-D) representation of the system where the aquifers are modeled as two-dimensional (2-D) or 3-D, while the aquitards are modeled as one-dimensional (1-D). This representation is usually adequate when the contrast in hydraulic conductivity between the aquitard and the aquifers is larger than two orders of magnitude causing groundwater flow in the aquitard to be mostly vertical (Neuman and Witherspoon 1969).

A challenge arises when the sediments comprising the aquitard units are extremely compressible, such as in the case of

✉ Eric Morales-Casique
ericmc@geologia.unam.mx

[1] Posgrado en Ciencias de la Tierra, Universidad Nacional Autónoma de México, C.P. 04510 Ciudad de México, Mexico

[2] Instituto de Geología, Universidad Nacional Autónoma de México, C.P. 04510 Ciudad de México, Mexico

[3] Instituto de Geofísica, Universidad Nacional Autónoma de México, C.P. 04510 Ciudad de México, Mexico

Author's personal copy

Mexico City (Marsal and Mazari 1959; Rudolph and Frind 1991; Ortega-Guerrero et al. 1999). Subsidence rates in the Basin of Mexico have exceeded 400 mm/year and more than 13.5 m of subsidence has accrued (Ortega-Guerrero et al. 1999; Auvinet 2009). Rates of nearly 350 mm/year have been measured recently (Cabral-Cano et al. 2008). Subsidence in this case is the result of large pumping rates and the highly compressible nature of the clayey materials, which are described as allophanes (Carreón-Freyre et al. 2010; Jaime-P and Méndez-Sánchez 2010). The poromechanical and physical properties of the media such as porosity, storativity (S_s) and hydraulic conductivity (K), are reduced during consolidation leading to a nonlinear groundwater flow equation. Helm (1976) developed a theory to model 1-D flow and consolidation accounting for stress-dependent K and S_s. Neuman et al. (1982) developed a quasi-3-D mathematical and numerical model that accounts for stress-dependent parameters in the aquitard. Rivera et al. (1991) developed a regional quasi 3-D model of the hydrogeologic system in Mexico City accounting for stress-dependent parameters in the aquitard; they divided the aquitard in layers with different properties. Rudolph and Frind (1991) developed a 1-D nonlinear groundwater flow and consolidation algorithm to simulate the behavior of highly compressible aquitards. The properties for their simulation cases where those typically observed in the compressible clay aquitard in Mexico City. Their results show that as hydraulic diffusivity (K/S_s) is reduced due to consolidation groundwater flow is also reduced leading to longer transient behavior and to less total land settlement than what is predicted by a lineal (stress-independent parameter) model. The algorithm of Rudolph and Frind (1991) was later applied to model subsidence in the Chalco region, in the metropolitan area of Mexico City (Ortega-Guerrero et al. 1999; Ortíz-Zamora and Ortega-Guerrero 2010).

The nonlinear models applied to Mexico City's aquitard employed either a constant distribution or smoothly variable distribution of initial parameters (Rudolph and Frind 1991; Ortega-Guerrero et al. 1999; Ortíz-Zamora and Ortega-Guerrero 2010), or a constant initial distribution by layers (Rivera et al. 1991); however, field data suggest that parameters, particularly porosity and K, are highly variable even in the vertical direction (Marsal and Mazari 1975; Vargas and Ortega-Guerrero 2004; Juárez-Camarena 2015). Figure 1a depicts the saturated gravimetric water content w in a geotechnical bore in the lacustrine aquitard in Mexico City; variations in w lead to void ratio ranging from 1 to 10. Vargas and Ortega-Guerrero (2004) conducted permeability tests in nests of piezometers in the aquitard of Mexico City and found that K is highly variable (Fig. 1b). Adequate representation of realistic parameter heterogeneity is recently being incorporated in groundwater flow and consolidation models. Frias et al. (2004) investigated the effect of random K in highly heterogeneous poroelastic reservoirs. Ferronato et al. (2006) employed Monte Carlo simulation to model regional land subsidence considering the vertical uniaxial rock compressibility as random. Stochastic poroelastic models are being developed (Wang and Hsu 2009, 2013); however, realistic parameter heterogeneity in highly compressible aquitards is yet to be included in groundwater flow and consolidation models.

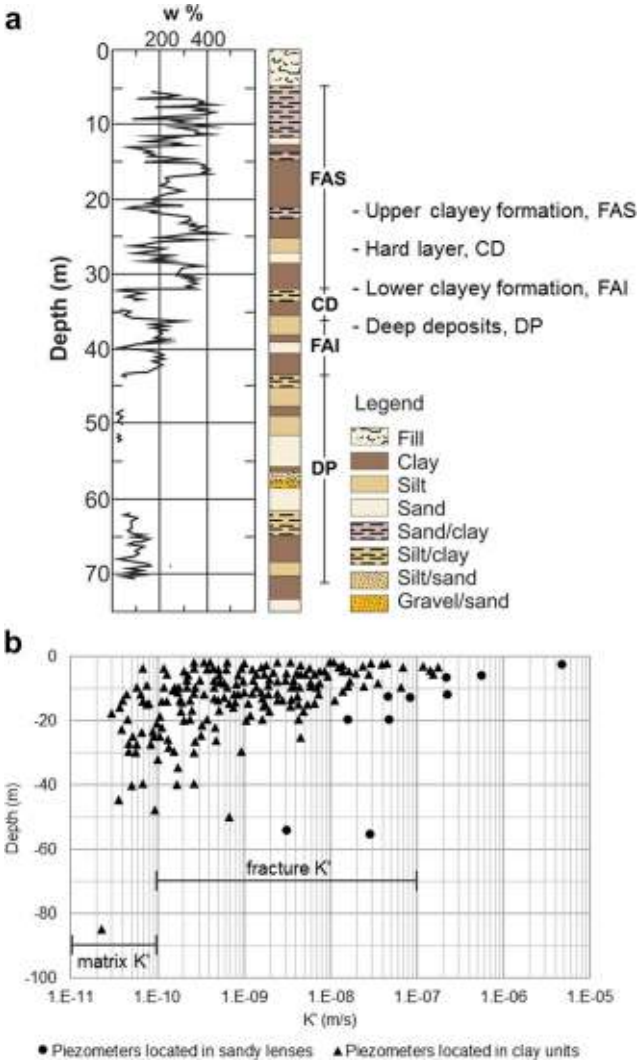

Fig. 1 **a** Gravimetric water content w at saturation in bore Pc 28 in Mexico City (Marsal and Mazari 1975), **b** hydraulic conductivity measured in several boreholes in the aquitard of Mexico City (Vargas and Ortega-Guerrero 2004)

In this paper, the effect of realistic vertical parameter heterogeneity in a nonlinear 1-D model of groundwater flow and consolidation is explored by means of Monte Carlo simulation. Since the focus is on the nonlinear consolidation of highly compressible aquitards, and for computational efficiency, the upper and lower aquifers are represented by known head (Dirichlet) boundaries. This is equivalent to assuming that flow from and to the aquitard does not alter the head of the upper and lower aquifers. The lower boundary is set to represent an instant drop in hydraulic head due to groundwater pumping. Realistic realizations of heterogeneous vertical distribution of parameters are generated based on a literature review in the highly compressible aquitard of Mexico City.

Author's personal copy

The numerical tests consider one random parameter at a time and leave the case where parameters are correlated for future research efforts. By employing a stochastic simulation framework, it is possible to identify which parameter or parameters lead to the largest effect on predicting land subsidence and the largest uncertainty associated to that prediction in these highly compressible systems. In the next section, the nonlinear groundwater flow and consolidation model, the literature review on vertical variability of parameters, the tests cases and the generation of random realizations are described. Next, the results of the numerical experiments are discussed as well as the effect on computed total settlement, groundwater fluxes and time to approximate steady state. Finally, the implications for more realistic simulation of land subsidence are discussed.

Materials and methods

Nonlinear subsidence algorithm

To model 1-D groundwater flow and nonlinear subsidence, the algorithm of Neuman et al. (1982), modified by Rudolph and Frind (1991), was employed. In a hydrogeological aquifer-aquitard-aquifer system, the focus is only on the consolidation of the aquitard, and for simplicity the system is decoupled and the effect of the aquifers is modeled as Dirichlet boundary conditions. Hence, the 1-D flow equation in the aquitard is given by:

$$\frac{\partial}{\partial z}\left[K(e)\frac{\partial h}{\partial z}\right] = S_s(e,\sigma_e)\frac{\partial h}{\partial t} \tag{1}$$

subject to

$$h(z,0) = h_0 \tag{2}$$

$$h(0,t) = h_1(t) \tag{3}$$

$$h(b,t) = h_2(t) \tag{4}$$

where h is hydraulic head (m), K is hydraulic conductivity (m/s), S_s is specific storage (1/m), b is the aquitard thickness (m) and $h_1(t)$ and $h_2(t)$ are hydraulic head in the lower and upper aquifers, respectively. The lateral extension of the aquitard is considered large enough for the 1-D representation to be valid.

Notation in Eq. (1) highlights that parameters K and S_s are functions of void ratio e and effective stress σ_e. In addition, a heterogeneous aquitard is considered and thus K and S_s are also functions of the spatial coordinate z. The algorithm adopts Terzaghi's 1-D consolidation theory (Terzaghi 1925). Assuming the total stress is constant and neglecting changes in z during the consolidation process leads to the following relation

$$\gamma \Delta h = -\Delta\sigma_e \tag{5}$$

where γ is specific weight of water (kg/m^3). Changes in σ_e will lead to changes in e. The relationship between an incremental change in the effective stress $d\sigma_e$ and the resulting change in the void ratio $de(\sigma_e)$ in the highly compressible stress range is expressed as (Rudolph and Frind 1991)

$$de(\sigma_e) = C_c \log\left(\frac{\sigma_{e_0} + d\sigma_e}{\sigma_{e_0}}\right) \tag{6}$$

where C_c is compression index (the negative slope of the e versus log σ_e curve) and σ_{e_0} is the initial effective stress (kN/m^2; Fig. 2).

The algorithm employs an empirical expression to relate hydraulic conductivity $dK(e)$ to changes in void ratio de (Rudolph and Frind 1991)

$$dK(e) = K_0(e)\left(10^{de/m} - 1\right) \tag{7}$$

where $K_0(e)$ is hydraulic conductivity at the start of the loading increment and m is the slope of an empirical linear relation between e and log K (Lambe and Whitman 1969; Fig. 3).

Specific storage as a function of effective stress and void ratio is computed by

$$S_s(e,\sigma_e) = \frac{\rho g C_c \log\left(\frac{\sigma_{e_0} + d\sigma_e}{\sigma_{e_0}}\right)}{d\sigma_e(1.0 + e_0)} \tag{8}$$

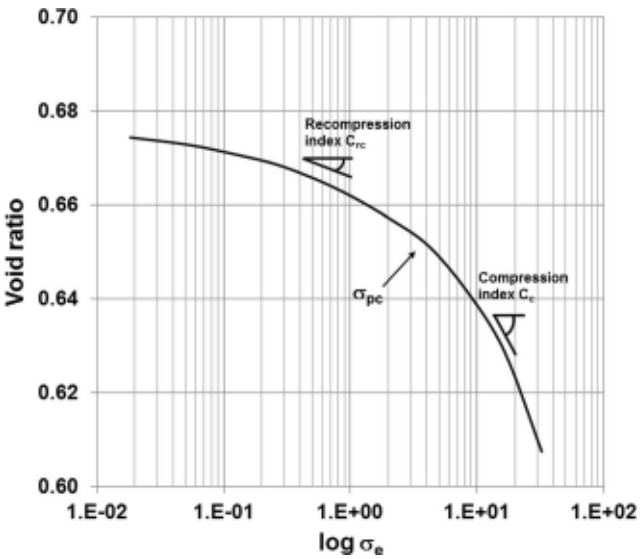

Fig. 2 Typical relation between effective stress and void ratio (Rudolph and Frind 1991)

Author's personal copy

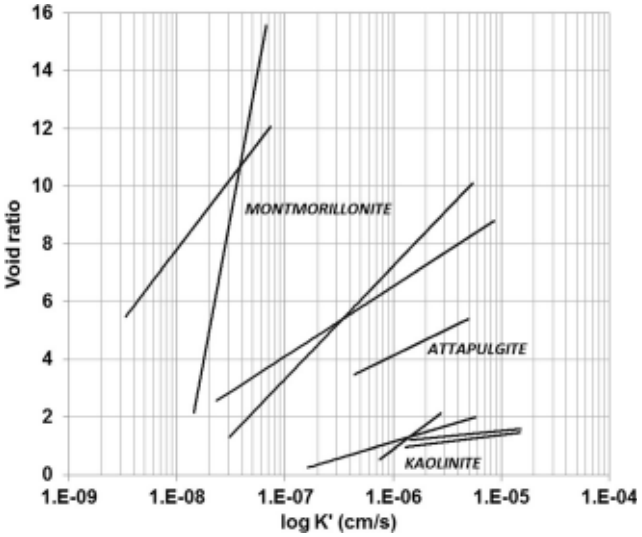

Fig. 3 Relation between log K and e (Lambe and Whitman 1969)

where ρ is water density (kg/m^3) and g is the gravity constant (m/s^2). Finally, deformation is computed by

$$dL_e = L_e\left(\frac{de}{1+e_0}\right) \tag{9}$$

where dL_e is the differential length change (m) and L_e is length of an element in a numerical mesh (m).

Test case: random heterogeneity

The effect of vertical heterogeneity on nonlinear subsidence is investigated in a synthetic hydrogeologic setting similar to the one employed by Rudolph and Frind (1991). The aquitard is 15 m thick and initial effective stress increases linearly with depth; preconsolidation stress is set to 15 kN/m^2. The aquitard is stressed by instantaneously lowering the pore pressure along the bottom boundary, simulating the effect of pumping in the lower aquifer. The geometry of the test case along with boundary conditions and initial distributions of σ_e, e, K and S_s are shown in Fig. 4. The initial distributions of σ_e, e, K and S_s were selected as in the generic case in Rudolph and Frind (1991), except that in the present case these spatial distributions represent ensemble means from which random realizations are generated.

The statistical data to design the numerical study were obtained from a literature review about the spatial variability of the parameters involved in the previous algorithm (namely K, e, C_c and m) in the highly compressible lacustrine aquitard in the Basin of Mexico (Fig. 5). The aquitard consists of lacustrine Quaternary sediments composed by montmorillonite, illite, kaolinite, halloysite and smectite, interbedded with volcanic material (Marsal and Mazari 1959; Peralta y Fabi 1989; Warren and Rudolph 1997; Díaz-Rodríguez et al. 1998) with a maximum thickness of about 300 m in the Chalco plain (Ortega-Guerrero et al. 1999).

With respect to K, Vargas and Ortega-Guerrero (2004) conducted 225 permeability tests at depths of 2–85 m in the previously mentioned aquitard. They found that K values range from 1×10^{-11} and 1×10^{-7} m/s and that log-Gaussian regression models can be fitted to the data. With respect to void ratio e, drillings for geotechnical investigations in the Mexico City aquitard have revealed a range of values from 2 to 12 (Marsal and Mazari 1959) and up to 15 (Juárez-Badillo and Rico-Rodríguez 2012). Values of compression index C_c depend on the type of clay and they have been found to be vertically variable in drillings for geotechnical investigations. Hernández-Marín et al. (2005) and Carreón-Freyre et al. (2006) report values of C_c ranging from 0.4 to 3.5. Carreón-Freyre et al. (2015) report values of C_c ranging from 0.1 to 3.5 in the western part of Mexico City. In a geotechnical study for the Metropolitan Cathedral in Mexico City, Covarrubias-Fernández (1994) found C_c values from 1.4 to 12.1. Finally, the slope m relating e and log K typically ranges from 0.02 to 10 (Lambe and Whitman 1969) for a variety of materials. For the aquitard in Mexico City, Covarrubias-Fernández (1994) found values of m ranging from 0.6 to 4; however, the aforementioned

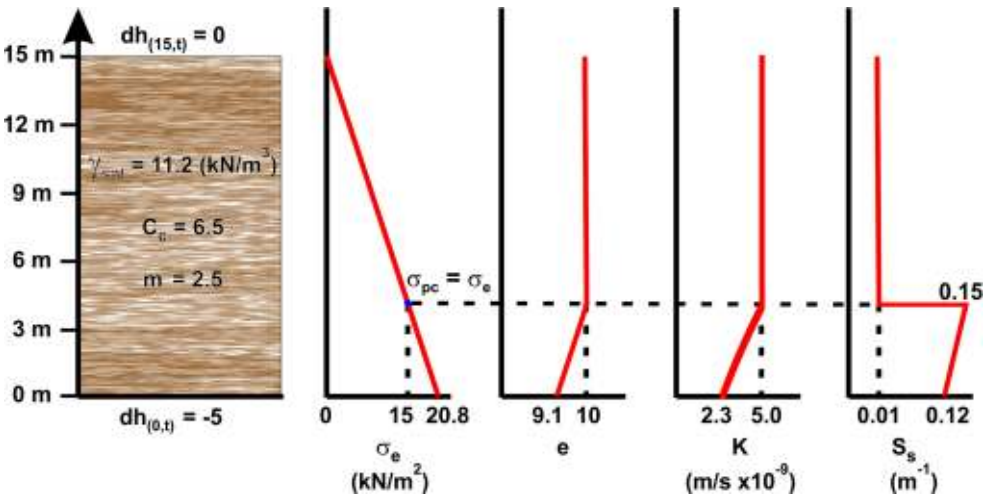

Fig. 4 Test case (adapted from Rudolph and Frind 1991)

Author's personal copy

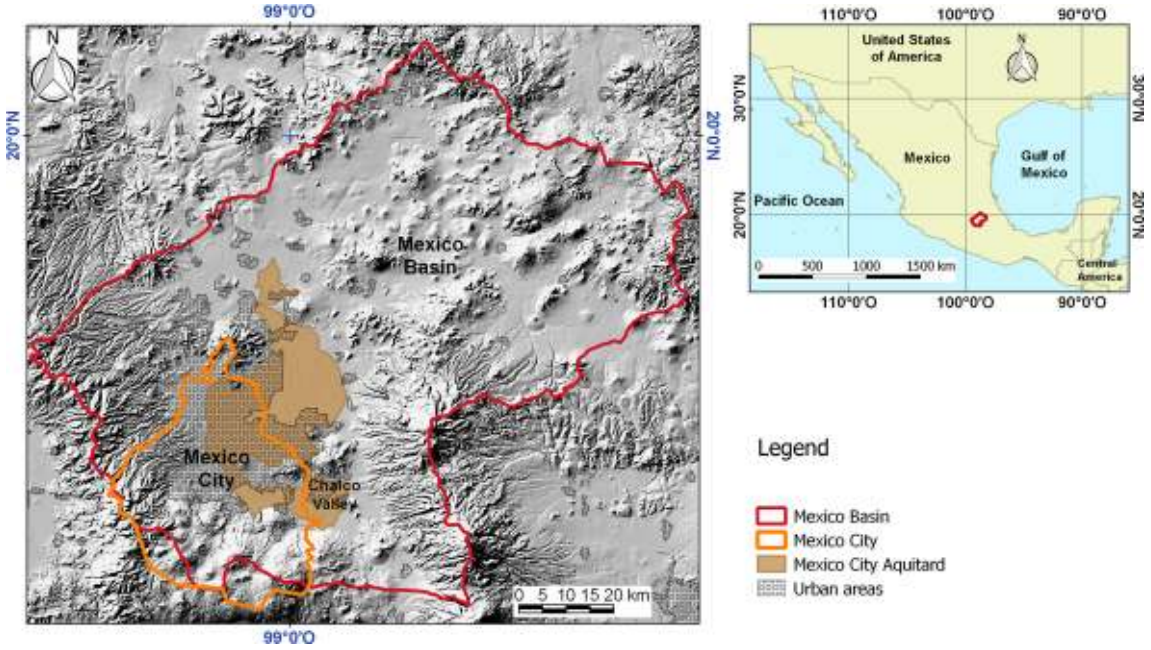

Fig. 5 Location of the Basin of Mexico (red line), Mexico City limits (orange line), urban area (gray-patterned polygon) and highly compressible lacustrine sediments (brown polygon)

studies did not conduct geostatistical analyses of the data. The only geostatistical analysis in the highly compressible sediments of the lacustrine aquitard of Mexico City was conducted by Juárez-Camarena (2015) who conducted a geostatiscal analysis of gravimetric water content w with data from geotechnical boreholes, after which he modeled w with an exponential correlation with a vertical integral scale of 2.1 m.

Table 1 summarizes the statistical data selected for each parameter. With this statistical data 2,000 realizations were generated employing sequential Gaussian simulation implemented in the package RandomFields (Schlather et al. 2016) implemented in R (R Core Team 2015). For simplicity, the focus is on one random parameter at a time keeping the rest deterministic (future work should study the effect of cross-correlation between parameters); thus, each parameter was simulated independently with zero mean and exponential covariance, where variance and integral scale are given in Table 1. In absence of geostatistical analyses that provide typical values of integral scales for each parameter in highly compressible aquitards, the integral scale is set to 2.1 (the value reported by Juárez-Camarena 2015). The resulting zero-mean realizations for each parameter were then scaled to fit the distribution in Fig. 4, representing a spatially variable mean. After the first set of numerical experiments, ln K was selected as the parameter with the largest effect on total settlement, and the effect of different variance and integral scale values for ln K was further investigated in an additional set of simulations.

Numerical solution

The 1-D groundwater flow and nonlinear consolidation algorithm is solved by implicit finite differences in a

Table 1 Statistical data selected for test case

Parameter	Correlation structure	Variance	Integral scale (m)	Reference
ln K	Exponential	4.01	2.1	Vargas and Ortega-Guerrero (2004); Juárez-Camarena (2015)
C_c	Exponential	5.37	2.1	Covarrubias-Fernández (1994); Juárez-Camarena (2015)
m	Exponential	0.88	2.1	Covarrubias-Fernández (1994); Juárez-Camarena (2015)
e	Exponential	3.22	2.1	Marsal and Mazari (1959); Covarrubias-Fernández (1994); Juárez-Camarena (2015)

Ensemble mean for each parameter is depicted in Fig. 4

Author's personal copy

deforming mesh (Eq. 9). The numerical scheme leads to a tridiagonal matrix and the algebraic equation is solved by the Thomas algorithm. The numerical mesh consists of 118 elements initially with $\Delta z = 0.127$ m. Total simulation time was selected as 275 years and was enough for most realizations to approximate steady state; however, many realizations of K required longer time to approximate steady state. Hence, all simulations for random K were also run for 1,000 years for adequate computation of ensemble moments. To deal with the nonlinearity in the parameters a predictor-corrector algorithm is implemented and the time step in all simulations is restricted to approximately 1 day to limit large changes in the parameters.

Results

In this section, the Monte Carlo simulation results for the cases with one random parameter will be presented first. Then the results of total settlement (subsidence) will be discussed. Finally, the flow through the aquitard and the time to reach steady state will be presented and discussed.

Random *K*

Figure 6a depicts 2,000 realizations of K (gray lines) with the ensemble average depicted by the blue line, which is the same as the distribution of K for the deterministic

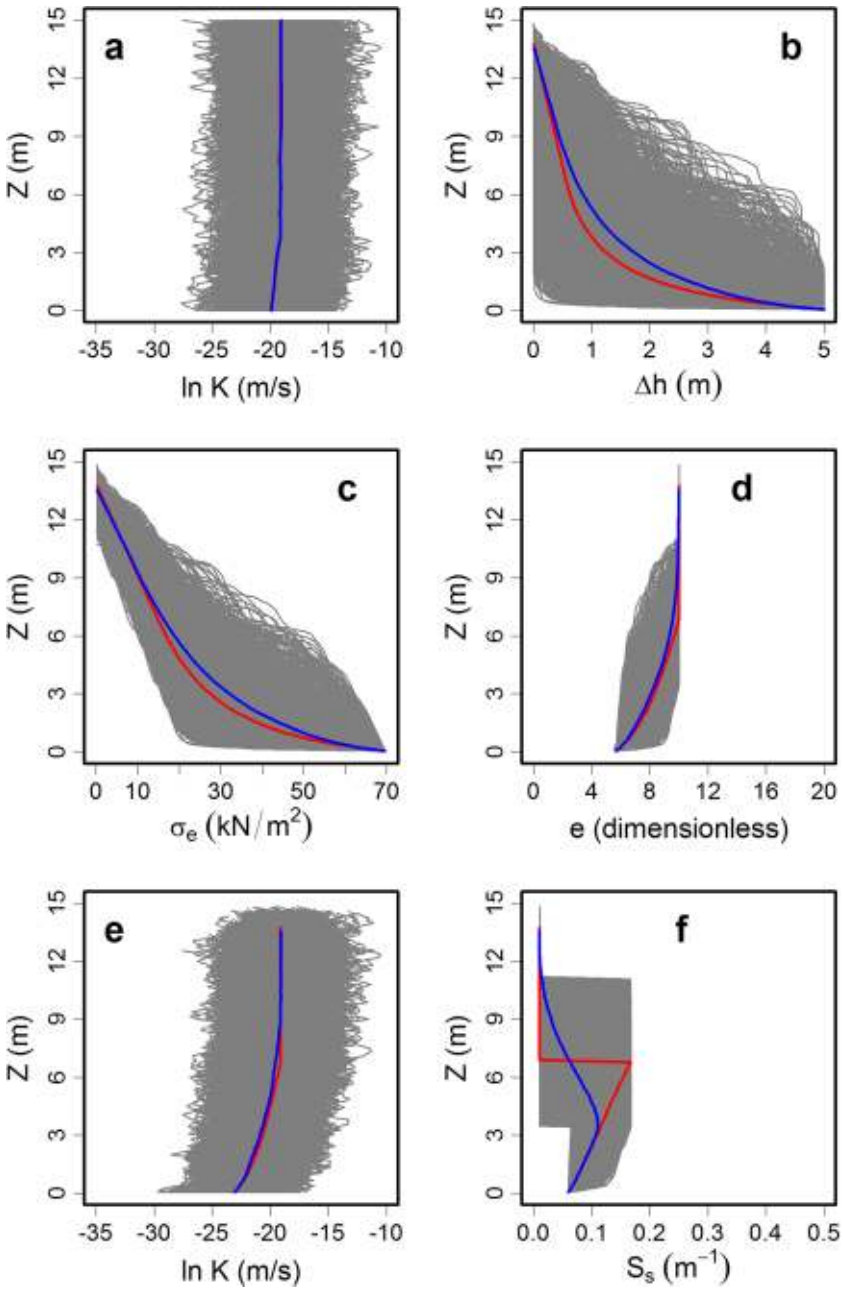

Fig. 6 Monte Carlo simulation results (gray lines) of groundwater flow and nonlinear consolidation considering K as a random field. The blue line is the ensemble average and the red line is the deterministic reference case. **a** Initial 2,000 realizations of K; **b**–**f** results at $t = 1{,}000$ years

Author's personal copy

reference case (Fig. 4). Also depicted are the simulation results at $t = 275$ years for change in hydraulic head (Fig. 6b), effective stress (Fig. 6c), void ratio e (Fig. 6d), K (Fig. 6e) and S_s (Fig. 6f). In each figure the ensemble average is depicted by a blue line, while the solution for the deterministic case is depicted by a red line. Figure 6 shows that the resulting ensemble averages differ from the deterministic reference case solution, except for K where both deterministic solution and ensemble average are similar. The deterministic case predicts smaller changes in Δh (hence underestimating changes in pore pressure) than the ensemble average, leading to similar behavior in effective stress. In turn, this leads to larger reduction in void ratio for the ensemble average than the deterministic case (Fig. 6d). The largest difference between the deterministic results and the ensemble average is seen in specific storage (Fig. 6f), where the latter is smoother. Single realizations of S_s exhibit the same behavior as the deterministic case; however, when averaging, the result exhibits a "smooth" shape that gets smoother as the dispersion in the realizations of S_s increases. In addition, there is significant spreading of the realizations around the ensemble averages. The impact of this spreading on the computed variance of total subsidence will be discussed latter.

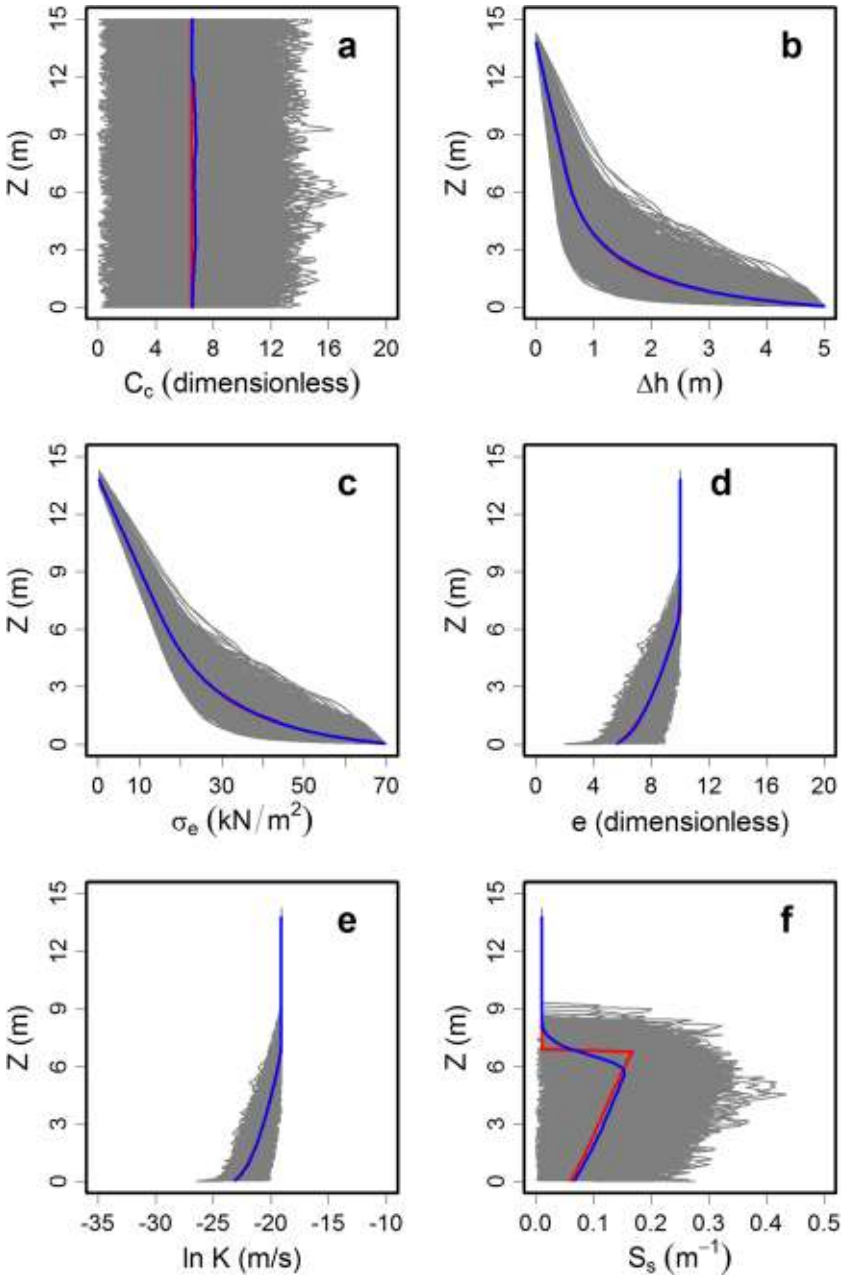

Fig. 7 Monte Carlo simulation results (gray lines) of groundwater flow and nonlinear consolidation considering C_c as a random field. The blue line is the ensemble average and the red line is the deterministic reference case. **a** Initial 2,000 realizations of C_c; **b**–**f** results at $t = 275$ years

Author's personal copy

Random C_c

The case of compression index C_c as a random variable is depicted in Fig. 7 where the results correspond to t = 275 years. The reference deterministic case assumes constant C_c (Fig. 4); thus, the ensemble average of the 2,000 realizations is constant (Fig. 7a). Contrasting with the previous case with random K, the case with random C_c leads to very similar results for the ensemble average (blue line) and the deterministic case (red line) for all variables and less spreading of the results for each realization (gray lines).

Random m

The case of m (the slope relating the empirical plot of log K and void ratio) as a random variable is depicted in Fig. 8 where the results correspond to t = 275 years. In this case, the ensemble average results are similar to the deterministic reference case, although the ensemble average of the drawdown is smaller than the drawdown in the deterministic case for z between 3–9 m (Fig. 8b). This leads to smaller ensemble averaged effective stress (Fig. 8c) and to larger ensemble average of void ratio (Fig. 8c), that is, smaller changes in void ratio with respect to the initial distribution. These differences

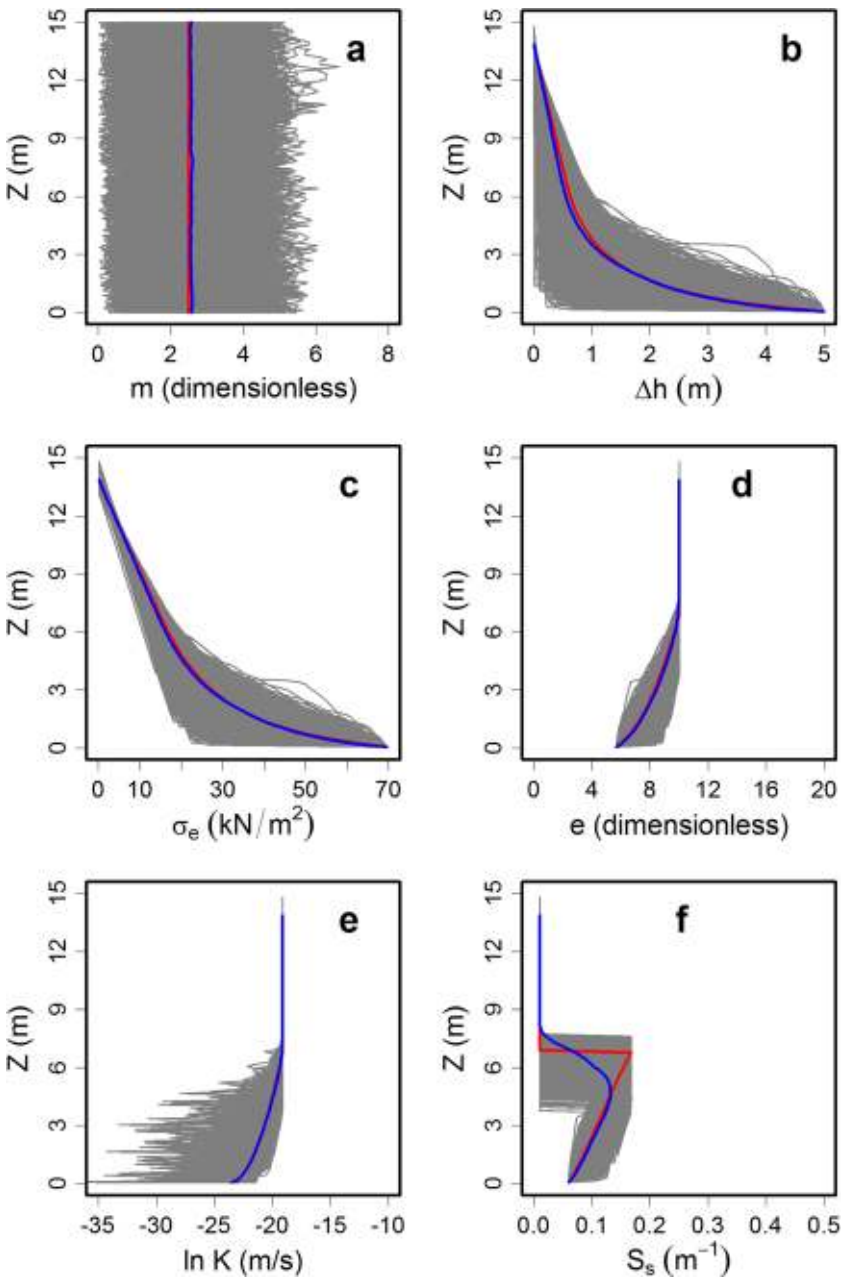

Fig. 8 Monte Carlo simulation results (gray lines) of groundwater flow and nonlinear consolidation considering m as a random field. The blue line is the ensemble average and the red line is the deterministic reference case. **a** Initial 2,000 realizations of m; **b**–**f** results at t = 275 years

Author's personal copy

between the ensemble average and the deterministic reference case are however smaller than those observed in the case of random K (Fig. 6). In addition, this case also leads to less spreading in the results for the 2,000 realizations than what is observed in the case of random K.

Random e

The final case considering void ratio e as a random variable is depicted in Fig. 9 for a total simulation time $t = 275$. In this case, the ensemble averages are very similar to the results of the deterministic reference case. In addition, this case resulted in minimum spreading of the 2,000 realizations results around the ensemble average of change in hydraulic head, effective stress and hydraulic conductivity (Fig. 9b,c,e, respectively). The main effect of random e is on the specific storage S_s (Fig. 9f).

Effect of parameter heterogeneity on total settlement

Figure 10 depicts the results for total settlement versus time corresponding to the four cases previously discussed: random K (Fig. 10a), random C_c (Fig. 10b), random m (Fig. 10c) and random e (Fig. 10d). Table 2 contains the ensemble average and variance of total settlement at the end of the simulation period of 275 years. The case of random K produces the largest differences in total settlement between the deterministic

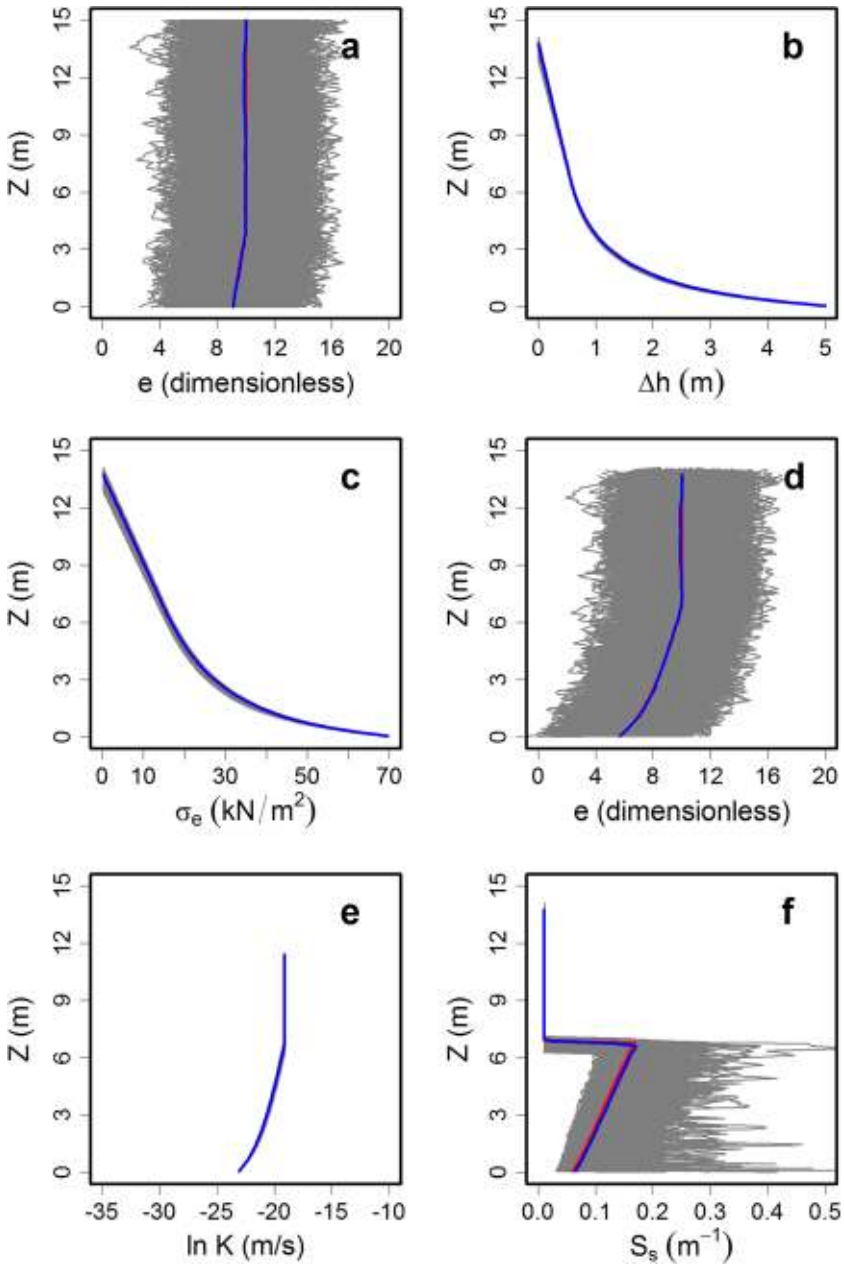

Fig. 9 Monte Carlo simulation results (gray lines) of groundwater flow and nonlinear consolidation considering e as a random field. The blue line is the ensemble average and the red line is the deterministic reference case. **a** Initial 2,000 realizations of e; **b**–**f** results at $t = 275$ years

Author's personal copy

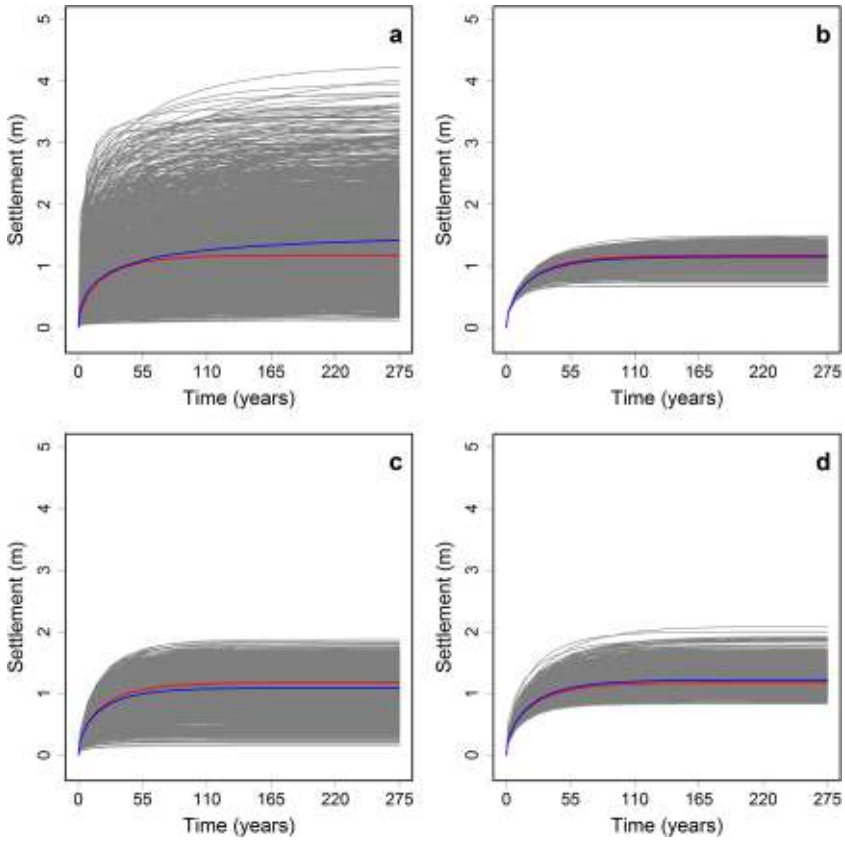

Fig. 10 Total settlement for **a** random K, **b** random C_c, **c** random m and **d** random e. The red line is the deterministic reference case, gray lines correspond to 2,000 Monte Carlo realizations and the blue line is the ensemble average of these realizations

case and the ensemble average; from 55 years on, the ensemble average significantly predicts larger settlement than the deterministic case. At the end of the simulation time, the total settlement for the deterministic case is 1.18 m, while the ensemble average is 1.42 m. Although the deterministic case reaches steady state after 168 years, the ensemble average of total settlement is still increasing after 275 years (Fig. 10a). In addition, random K also produces the largest spreading around the ensemble average of total settlement for individual realizations; some realizations produce total settlement at the end of the simulation time larger than 3 m. Variance of total settlement at $t = 275$ years is 0.51 m^2, the largest among the four cases considered.

The case with random m is the next parameter with the largest impact on the ensemble average of total settlement and on individual realizations. In this case, the ensemble average of total settlement is smaller than the corresponding prediction for the deterministic case; at $t = 275$ years the ensemble average of total settlement is 1.09 m and the variance is 0.1 m^2. The cases with random void ratio e and random C_c result in ensemble averages of total settlement of 1.22 and 1.15 m, respectively, which are values close to the 1.18 m of total settlement in the deterministic case. In addition, considering these two parameters as random results in low variance of total settlement at $t = 275$ years variance is 0.03 m^2 for random e and 0.02 m^2 for random C_c. From these results, it

Table 2 Ensemble average and variance of total settlement, boundary flux at 275 years, and time elapsed for the difference between top and bottom boundary fluxes being less than 1%. σ^2 = variance

Case	Total settlement		Boundary flux		Time to steady state	
	(m)	σ^2 (m2)	(mm/d)	σ^2(mm/d)^2	(years)	σ^2 (years^2)
Deterministic	1.18	–	0.034	–	168.00	–
Random K	1.42	0.51	~0.020	$\sim 1 \times 10^{-3}$	> 275	a
Random C_c	1.15	0.02	0.033	5.80×10^{-5}	169.40	1,503.36
Random m	1.09	0.10	0.029	1.16×10^{-4}	159.80	550.80
Random e	1.22	0.03	0.034	5.36×10^{-7}	170.40	396.03

[a] Boundary fluxes in a significant number of realizations still differed in more than 1% at the extended simulation time of 1000 years, thus their variance was not computed

Author's personal copy

is clear that the spatial variability of K produces the largest impact on total settlement and should be considered in simulating land subsidence. Correlation between random variables and its effect on consolidation will be considered in future work.

Flux at the boundaries

Figure 11 depicts the flux at the upper and lower boundaries versus time for the cases with random K (Fig. 11a), random C_c (Fig. 11b), random m (Fig. 11c) and random e (Fig. 11d). Table 2 contains the ensemble average and variance of boundary flux at the end of the simulation period of 275 years. At early simulation time, the flux at the $z = 0$ boundary reaches its maximum value, while flux at the top boundary is close to zero. As time progresses the flux at the bottom boundary diminishes, while the flux at the top boundary increases, both tending to a constant flux value. The time elapsed for the difference between the fluxes at the top and bottom boundaries to be less than 1% (to approximate steady state) is also presented in Table 2. At $t = 275$ years the flux at the top and bottom boundaries for the deterministic case is 0.034 mm/d; both fluxes are within 1% difference after 168 years. With respect to the case with random K, at $t = 275$ years the ensemble average of fluxes at the top and bottom boundaries are close to 0.02 mm/d but still with a difference larger than 1% between them; however, by extending the simulation time to 1,000 years, it was possible to verify that boundary fluxes differ in less than 1% after 525 years. In addition, boundary fluxes for each realization show significant spreading with a variance of 1×10^{-3} mm^2/d^2 at $t = 275$ years.

The case with random m resulted in an ensemble average of fluxes at the top and bottom boundaries of 0.029 mm/d and a flux variance of 1.16×10^{-4} mm^2/d^2 at $t = 275$ years. The case with random C_c resulted in an ensemble average of fluxes at the top and bottom boundaries of 0.033 mm/d and a flux variance of 5.8×10^{-5} mm^2/d^2 at $t = 275$ years. Finally, the case with random e resulted in an ensemble average of fluxes at the top and bottom boundaries of 0.034 mm/d and the smallest flux variance among the four cases, 5.36×10^{-7} mm^2/d^2 at $t = 275$ years. Time for the boundary fluxes to be within 1% difference ranged from 159.8 years for random m to 170.4 for random e (Table 2), while the largest variance was for random C_c and the smallest for random e. These results show that K is the parameter with the largest effect on total settlement and boundary fluxes.

Effect of variance, integral scale and correlation structure of random K on total settlement

In the previous section it was shown that the effect of random hydraulic conductivity has more impact on ensemble average

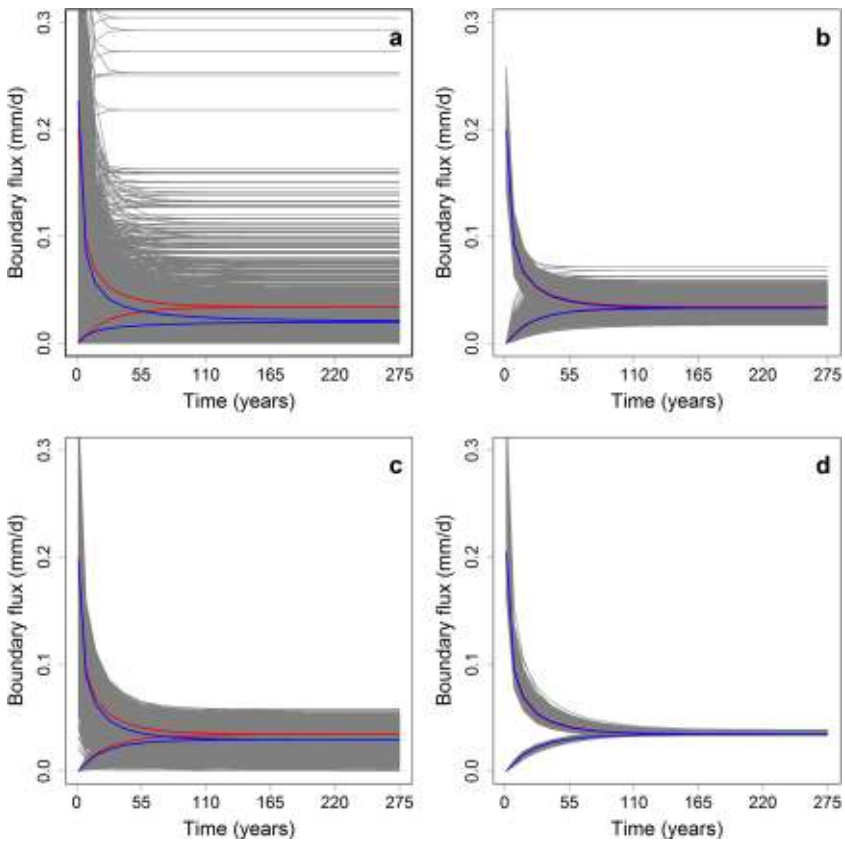

Fig. 11 Flux at the top and bottom boundaries for **a** random K, **b** random C_c, **c** random m and **d** random e. The red line is the deterministic reference case, gray lines correspond to 2,000 Monte Carlo realizations and the blue line is the ensemble average of these realizations

Author's personal copy

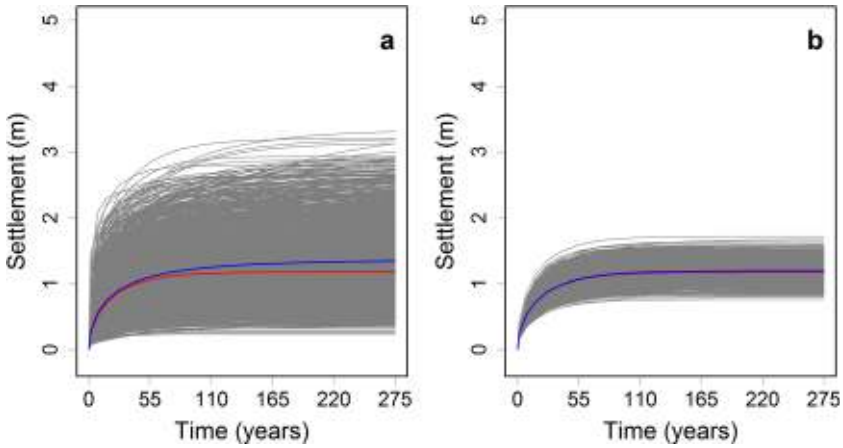

Fig. 12 Total settlement for **a** random K with logarithmic variance of 1.68 m^2/s^2 and **b** random K with logarithmic variance of 0.10 m^2/s^2. Red line is the deterministic reference case, gray lines correspond to 2,000 Monte Carlo realizations and blue line is the ensemble average of these realizations

total settlement predictions than the other three parameters considered. In this section the effect of two different values of variance of ln K: 1.68 m^2/s^2 (equal to the variance of C_c in the previous numerical example), and 0.10 m^2/s^2, is explored. In each case, 2,000 Monte Carlo realizations of ln K were generated and the nonlinear subsidence algorithm was run to 275 years.

Figure 12 depicts the results of total settlement versus time for both cases. Figure 12a depicts the results for total settlement considering random ln K with variance of 1.68 m^2/s^2. The ensemble average (blue line) is again larger than the deterministic results (red line), and at the end of the simulation this difference depicts an increase of 14% with 1.34 m of total settlement and variance of 0.27 m^2. Figure 12b depicts the results for ln K variance of 0.1 m^2/s^2. In this case the ensemble average (blue line) almost matches with the deterministic results (red line), with a low difference of 0.02 m that corresponds to a 1% increase with a settlement variance of 0.02 m^2 at the end of simulation. Comparing these results with those of the previous section (Table 2), if the variance of ln K is equal to the variance of C_c, the former case leads to larger ensemble total settlement (1.34 m) and larger variance (0.27 m^2) than the case with random C_c (ensemble total settlement of 1.15 m and variance of 0.02 m^2, Table 2). The effect of C_c is comparable to that of K when the variance of ln K is 0.1 m^2/s^2 (lower than the variance of C_c). These results support those in Table 2 and the observation that heterogeneity of K must be considered when modeling nonlinear consolidation in highly compressible aquitards.

Next the effect of varying the integral scale of ln K is explored; Fig. 13a depicts the results for an integral scale of 5 m, while Fig. 13b depicts the results for an integral scale of 10 m. In the first case, ensemble average total settlement is 1.41 m (20% larger than the deterministic case) with a variance of 0.60 m^2 at the end of the simulation. In the second case, integral scale of 10 m, the ensemble average total settlement is 1.31 m (12% larger than the deterministic case) with a variance of 0.52 m^2 at the end of the simulation. These results show that the ensemble average total settlement diminishes as the integral scale increases.

Finally, the impact of the correlation structure of ln K on total settlement is explored. Figure 14 depicts the total settlement versus time when ln K has a spherical correlation structure. In this case the magnitude of the ensemble average of total settlement (blue line) is smaller than the deterministic results (red line) at early times but larger at late times, contrasting with the results with an exponential covariance

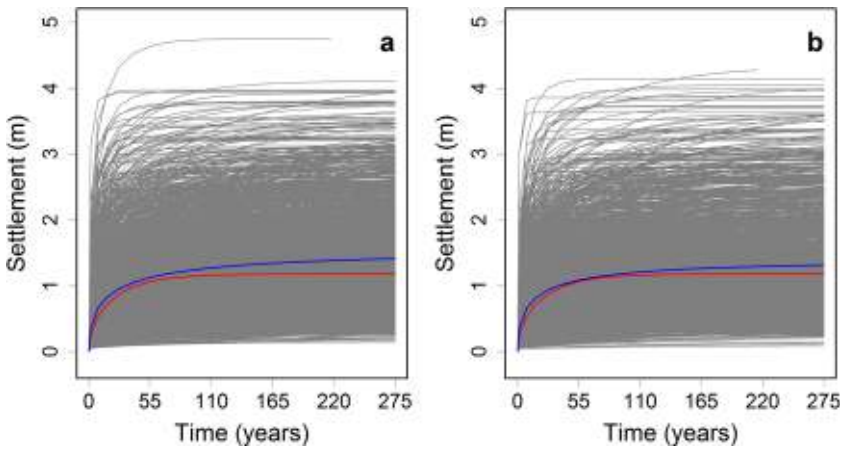

Fig. 13 Total settlement for ln K with integral scale of **a** 5 m and **b** 10 m. Red line is the deterministic reference case, gray lines correspond to 2,000 Monte Carlo realizations and blue line is the ensemble average of these realizations

Author's personal copy

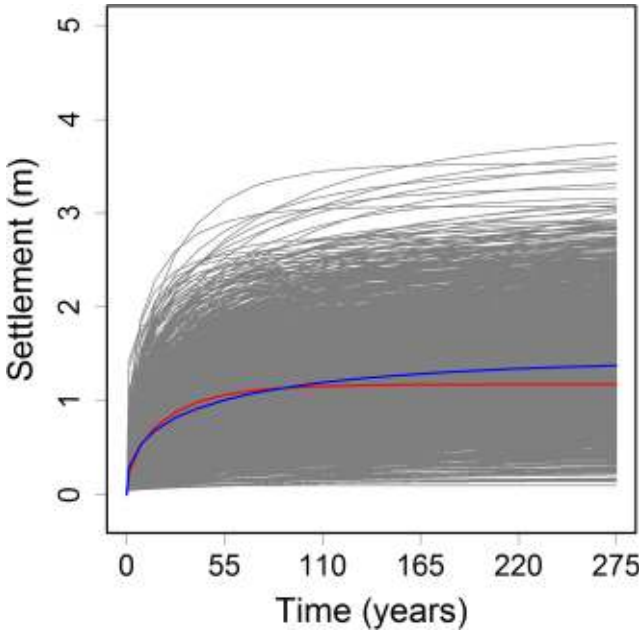

Fig. 14 Total settlement for random K with spherical correlation structure. Red line is the deterministic reference case, gray lines correspond to 2,000 Monte Carlo realizations and blue line is the ensemble average of these realizations

(Fig. 10a) where the ensemble average is always larger than the deterministic results. The ensemble average total settlement at the end of the simulation is 1.38 m (17% larger than total settlement for the deterministic case) with a variance of 0.35 m^2 (smaller than the case for exponential correlation structure, Table 2).

Conclusions

The effect of vertical heterogeneity in simulating nonlinear 1-D groundwater flow and consolidation in highly compressible aquitards was explored by means of Monte Carlo numerical simulation. Hydraulic conductivity K, compression index C_c, void ratio e and m (an empirical parameter relating K and e) were treated as independent, spatially correlated multi-Gaussian random variables. The results were expressed in terms of the ensemble average of the variables and compared to the results of a reference case with deterministic parameters.

The results of the numerical Monte Carlo simulations indicate that K has the largest impact on the nonlinear 1-D groundwater flow and consolidation. When compared to the reference case for a total simulation time of 275 years, the case with random K leads to 20% larger total settlement and about 40% less flux at the boundaries. While the deterministic case reaches steady state after 168 years, the ensemble averages of total settlement and boundary fluxes of the random case approximate steady state after 525 years. Parameter m is the second random variable in importance, probably due to its relation to K, leading to 7% less total settlement and 15% less boundary flux than the deterministic reference case. Considering compression index and void ratio as random variables leads to ensemble averages of total settlement and flux at the boundaries similar to the results of the deterministic reference case.

The case with random K also leads to the largest variance in all variables, including hydraulic head, effective stress, total settlement and boundary fluxes. Random K leads to variance for total settlement 5–25 times larger than the corresponding results considering m, C_c or e as random. Although each realization has a spatial mean similar to the deterministic case, total settlement can be very variable, between a few centimeters up to 2.85 m at 275 years (two times the standard deviation). Random K also leads to the largest variance in boundary fluxes and time to reach steady state.

These results highlight the fact that heterogeneity in K leads to the largest uncertainty in the prediction of consolidation in highly compressible aquitards. Inaccurate characterization of the aquifer system at the level of identifying aquitards, their hydromechanical properties and their heterogeneity may lead to significant errors in site-specific, predictive modeling. These results are based on a 1-D model. Variance of hydraulic head in heterogeneous 1-D models is typically smaller than what is obtained from two-dimensional (2-D) simulations. Therefore, total settlement and its variance in 2-D heterogeneous aquitards might be smaller than our results. However, this may not be enough to invalidate the main result: that spatial variability of K needs to be accounted for (in addition to variability of the other parameters) in modeling consolidation in these highly compressible systems. Future work should consider the case with cross-correlation between the parameters, 2-D and 3-D simulations and fully coupled aquitard-aquifer simulation.

Funding Information This research was funded by grant IN113717 from UNAM-DGAPA-PAPIIT and by a doctoral scholarship from CONACYT to the leading author.

References

Auvinet G (2009) Land subsidence in Mexico City. In: Auvinet GY, Juárez M (eds) Geotechnical engineering in urban areas affected by land subsidence. Volume prepared by ISSMGE Technical Committee 36 for XVII ISSMGE Conference, Alexandria, Egypt, 2009. Mexican Society of Soil Mechanics, Mexico City, pp 3–11

Burbey TJ (2005) Use of vertical and horizontal deformation data with inverse models to quantify parameters during aquifer testing. Proceedings of the 7th International Symposium on Land Subsidence, vol 2. Shanghai, October 2005, pp 560–569

Burbey TJ, Helm DC (1999) Modeling three-dimensional deformation in response to pumping of unconsolidated aquifers. Env Eng Geosci 5: 199–212

Cabral-Cano E, Dixon TH, Miralles-Wilhelm F, Díaz-Molina O, Sánchez-Zamora O, Carande RE (2008) Space geodetic imaging

Author's personal copy

of rapid ground subsidence in Mexico City. GSA Bull 120(11–12): 1556–1566

Carreón-Freyre DC, Hidalgo-Moreno CM, Hernández-Marín M (2006) Mecanismos de fracturamiento de depósitos arcillosos en zonas urbanas: caso de deformación diferencial en Chalco, Estado de México [Fracturing mechanisms of clay deposits in urban areas: case of differential deformation in Chalco, State of Mexico]. Bol Soc Geol Mexicana 57(2):237–250

Carreón-Freyre D, Cerca M, Galloway DL, Silva-Corona JJ (eds) (2010) Land subsidence, associated hazards and the role of natural resources development. IAHS Publ. 339, IAHS, Wallingford, UK

Carreón-Freyre D, González-Hernández M, Martinez-Alfaro D, Solís-Valdéz S, Cerca M, Millán-Malo B, Centeno-Salas F (2015) Analysis of the variation of the compressibility index (Cc) of volcanic clays and its application to estimate subsidence in lacustrine áreas. Proc ISHS 372: 273–279. https://doi.org/10.5194/piahs-372-273-2015

Covarrubias-Fernández S (1994) Characterization of the engineering properties of Mexico City clay. MSc Thesis, MIT, Cambridge, MA

Cruickshank-Villanueva C (1984) Numerical simulation of subsidence due to pumping with hysteresis effect included. Proceedings of the 3rd International Symposium on Land Subsidence, Venice, March 1984, Issue 151, pp 79–88

Díaz-Rodríguez JA, Lozano-Santa Cruz R, Dávila-Alcocer VM, Vallejo E, Girón P (1998) Physical, chemical, and mineralogical properties of Mexico City sediments: a geotechnical perspective. Can Geotech J 35(4):600–610

Ferronato M, Gambolati G, Teatini P, Baù D (2006) Stochastic poromechanical modeling of anthropogenic land subsidence. Int J Solids Struct 43:3324–3336. https://doi.org/10.1016/j.ijsolstr.2005.06.090

Frias DG, Murad MA, Pereira F (2004) Stochastic computational modelling of highly heterogeneous poroelastic media with log-range correlations. Int J Numer Anal Meth Geomech 28:1–32. https://doi.org/10.1002/nag.323

Galloway DL, Burbey TJ (2011) Review: Regional land subsidence accompanying groundwater extraction. Hydrogeol J 19(8):1459–1486. https://doi.org/10.1007/s10040-011-0775-5

Gambolati G, Freeze RA (1973) Mathematical simulation of the subsidence of Venice, 1: theory. Water Resour Res 9(3):721–733. https://doi.org/10.1029/91WR01567

Helm DC (1972) Simulation of aquitard compaction due to changes in stress. Trans Am Geophys Union 53(11):979, abstracts

Helm DC (1975) One-dimensional simulation of aquifer system compaction near Pixley, California: 1. constant parameters. Water Resour Res 11(3):465–478. https://doi.org/10.1029/WR011i003p00465

Helm DC (1976) One-dimensional simulation of aquifer system compaction near Pixley, California: 2. stress-dependent parameters. Water Resour Res 12(3):375–391. https://doi.org/10.1029/WR012i003p00375

Hernández-Marín M, Carreón-Freyre DC, Cerca M (2005) Mechanical and physical properties of the montmorillonitic and allophanic clays in the near-surface sediments of Chalco Valley, Mexico: analysis of contributing factors to land subsidence. In: Zhang A, Gong S, Carbognin L and AI Johnson (eds) Proceedings of the Seventh International Symposium on Land Subsidence, Shanghai, China.

Herrera I (1970) Theory of multiple leaky aquifers. Water Resour Res 6(1):185–193. https://doi.org/10.1029/WR006i001p00185

Herrera I, Figueroa VGE (1969) A correspondence principle for the theory of leaky aquifers. Water Resour Res 5(4):900–904. https://doi.org/10.1029/WR005i004p00900

Herrera I, Rodarte L (1973) Integrodifferential equations for systems of leaky aquifers and applications: 1. the nature of approximate theories. Water Resour Res 9(4):995–1005. https://doi.org/10.1029/WR009i004p00995

Hsieh PA, (1996) Deformation-Induced Changes in Hydraulic Head During Ground-Water Withdrawal. Ground Water 34(6):1082–1089. https://doi.org/10.1111/j.1745-6584.1996.tb02174.x

Herrera I, Yates R (1977) Integrodifferential equations for systems of leaky aquifers and applications: 3. a numerical method of unlimited applicability. Water Resour Res 13:725–732. https://doi.org/10.1029/WR013i004p00725

Jaime-P A, Méndez-Sánchez E (2010) Evolution of Mexico City clay properties affected by land subsidence. In: Carreón-Freyre D, Cerca M, Galloway DL, Silva-Corona JJ (eds) Land subsidence, associated hazards and the role of natural resources development. IAHS Publ. 339, IAHS, Wallingford, UK, pp 232–234

Juárez-Badillo E, Rico-Rodríguez A (2012) Mecánica de suelos, tomo 1: fundamentos de la Mecánica de Suelos [Soil mechanics, vol 1: fundamentals of Soil Mechanics]. Limusa, Durban, South Africa

Juárez-Camarena M (2015) Análisis geoestadístico del subsuelo de la zona lacustre del Valle de México [Geostatistical analysis of the subsoil in the lacustrine areas of the Valley of Mexico]. PhD Thesis, UNAM, Mexico City

Lambe TW, Whitman RV (1969) Soil mechanics, series in soil engineering. Wiley, Chichester, UK

Marsal RJ, Mazari M (1959) El subsuelo de la Ciudad de México [The subsoil of Mexico City]. Facultad de Ingeniería, Universidad Nacional Autónoma de México, Mexico City

Marsal RJ, Mazari M (1975) The lacustrine clays of the Valley of Mexico. Universidad Nacional Autónoma de México, Mexico City

Meade RH (1967) Petrology of sediments underlying areas of land subsidence in central California. US Government Printing Office, Washington, DC

Narasimhan TN, Witherspoon PA (1977) Numerical model for land subsidence in shallow groundwater systems. Proceedings of the Second International Symposium on Land Subsidence, Anaheim, CA, December 1976, IAHS Publ. 121, IAHS, Wallingford, UK, pp 133–144

Neuman SP, Witherspoon PA (1969) Transient flow of ground water to wells in multiple-aquifer systems. Geotechnical engineering report, University of California, Berkeley, CA

Neuman SP, Preller C, Narasimhan TN (1982) Adaptative explicit-implicit quasi three-dimensional finite element model of flow and subsidence in multiaquifer systems. Water Resour Res 18(5):1551–1561. https://doi.org/10.1029/WR018i005p01551

Ortega-Guerrero A, Rudolph DL, Cherry JA (1999) Analysis of long-term land subsidence near Mexico City: field investigations and predictive modeling. Water Resour Res 35(11):3327–3341. https://doi.org/10.1029/1999WR900148

Ortíz-Zamora D, Ortega-Guerrero A (2010) Evolution of long-term land subsidence near Mexico City: review, field investigations, and predictive simulations. Water Resour Res 46(1). https://doi.org/10.1029/2008WR007398

Peralta y Fabi R (1989) Sobre el origen de algunas propiedades mecánicas de la formación arcillosa superior del Valle de México [On the origin of some mechanical properties of the upper clay formation in the Valley of Mexico]. Simposio sobre Tópicos Geológicos de la Cuenca del Valle de México [Symposium on geological topics of the Basin of Mexico], Sociedad Mexicana de Mecánica de Suelos, Mexico City

Poland JF, Davis GH (1969) Land subsidence due to withdrawal of fluids. Rev Eng Geol 2:187–269

R Core Team (2015) R: a language and environment for statistical computing. R Foundation for Statistical Computing, Vienna, Austria. https://www.r-project.org/. Accessed April 2015

Rivera A, Ledoux E, De Marsily G (1991) Nonlinear modeling of groundwater flow and total subsidence of the Mexico City aquifer-aquitard system. Proceedings of the Fourth International Symposium on Land Subsidence, Houston, TX, May 1991

Author's personal copy

Rudolph DL, Frind EO (1991) Hydraulic response of highly compressible aquitards during consolidation. Water Resour Res 27(1):17–30. https://doi.org/10.1029/90WR01700

Sandhu RS (1979) Modeling land subsidence. ASCE, Washington, DC

Schlather M, Malinowski A, Oesting M, Boecker D, Strokorb K, Engelke S, Martini J, Ballani F, Moreva O, Auel J, Menck PJ, Gross S, Ober U, Berreth C, Burmeister K, Manitz J, Ribeiro P, Singleton R, Pfaff B, R Core Team (2016) RandomFields: simulation and analysis of random fields. R package version 3.1.8. https://cran.r-project.org/package=RandomFields. Accessed November 2017

Terzaghi K (1925) Principles of soil mechanics, IV: settlement and consolidation of clay. Eng News-Record 95(3):874–878

Vargas C, Ortega-Guerrero A (2004) Fracture hydraulic conductivity in the Mexico City clayey aquitard: field piezometer rising-head tests. Hydrogeol J 12(3):336–344. https://doi.org/10.1007/s10040-003-0302-4

Verruijt A (1969) Elastic storage of aquifers. In: Flow through porous media. Academic, San Diego, CA, pp 331–376

Wang SJ, Hsu KC (2009) Dynamics of deformation and water flow in heterogeneous porous media and its impact on soil properties. Hydrol Process 23:3569–3582. https://doi.org/10.1002/hyp.7458

Wang SJ, Hsu KC (2013) Dynamic interactions of groundwater flow and soil deformation in randomly heterogeneous porous media. J Hydrol 499:50–60. https://doi.org/10.1016/j.jhydrol.2013.06.047

Warren CJ, Rudolph DL (1997) Clay minerals in basin of Mexico lacustrine sediments and their influence on ion mobility in groundwater. J Contam Hydrol 27(3-4):177–198

Witherspoon PA, Freeze RA (1972) The role of aquitards in multiple-aquifer systems. Eos Trans Am Geophys Union 53(7):743–746. https://doi.org/10.1029/EO053i007p00743